Research Square

Preprints are preliminary reports that have not undergone peer review.
They should not be considered conclusive, used to inform clinical practice,
or referenced by the media as validated information.

Diversity and Pathogenicity of Colletotrichum Species Associated with Walnut Anthracnose in Northern Italy

Salvatore Iacono
University of Bologna
Laura Luongo
Council for Agricultural Research and Economics-Plant Protection and Certification-Rome
Andrea Menicucci
University of Bologna
Ivana Garaguso
Council for Agricultural Research and Economics-Plant Protection and Certification-Rome
Irene Belleggia
University of Bologna
Riccardo Bugiani
Regione Emilia-Romagna
Riccardo Baroncelli
University of Bologna
Salvatore Vitale
salvatore.vitale@crea.gov.it

Council for Agricultural Research and Economics-Plant Protection and Certification-Rome

Article

Keywords: Juglans regia, anthracnose, Colletotrichum, phylogenomics, multilocus sequence typing, pathogenicity.

Posted Date: November 24th, 2026

DOI: https://doi.org/10.21203/rs.3.rs-11375034/v1

License: This work is licensed under a Creative Commons Attribution 4.0 International License.
Read Full License

Additional Declarations:

No competing interests reported.

Figure 7 are not available with this version.

Diversity and Pathogenicity of Colletotrichum Species Associated with Walnut Anthracnose in Northern Italy

Salvatore Iacono[1*], Laura Luongo[2*], Andrea Menicucci[1], Ivana Garaguso[2], Irene Belleggia[1], Riccardo Bugiani[4,] Riccardo Baroncelli[1,3,] Salvatore Vitale[2]

[1]Department of Agricultural and Food Sciences, University of Bologna, 40127, Bologna, Italy,

[2]Council for Agricultural Research and Economics-Plant Protection and Certification-Rome, Italy,

[3]Center for Studies on Bioinspired Agro-Enviromental Technology, University of Naples Federico II, 80055, Portici, Italy

[4]Plant Protection Service, Emilia-Romagna Region, Via Saliceto 81, 40128 Bologna, Italy

*Salvatore Iacono and Laura Luongo contributed equally to this work

Corresponding author: Salvatore Vitale salvatore.vitale@crea.gov.it

Abstract

Walnut anthracnose has emerged as an important disease affecting intensive walnut production systems worldwide. Although several *Colletotrichum* species have recently been associated with walnut anthracnose, information on their diversity and distribution in Europe remains limited. In this study, a large-scale survey was conducted between 2016 and 2024 in commercial walnut orchards in Northern Italy to investigate the diversity, phylogenetic relationships, and pathogenicity of walnut-associated *Colletotrichum* species. Forty-four isolates obtained from nuts, buds, stigmas, and leaves were characterized using morphology, multilocus sequence typing (MLST), whole-genome sequencing, phylogenomics, and pathogenicity assays. MLST analyses identified six species belonging to three species complexes: *C. fioriniae*, *C. nymphaeae*, and *C. godetiae* within the *C. acutatum* species complex; *C. fructicola* and *C. siamense* within the *C. gloeosporioides* species complex; and *C. sojae* within the *C. orchidearum* species complex. Phylogenomic analyses based on 18 newly sequenced genomes confirmed all species assignments obtained through MLST and provided genome-scale support for species delimitation. Pathogenicity assays showed that representative isolates of all six species induced lesions on artificially wounded walnut fruits. Lesion sizes differed among tested isolates, with the *C. nymphaeae isolate* producing the largest lesions under the experimental conditions. Notably, *C. fructicola*, *C. siamense*, and *C. sojae* are reported here for the first time as causal agents of walnut anthracnose in Europe.

These findings expand the known diversity of walnut-associated *Colletotrichum* species and provide genomic resources for future epidemiological and evolutionary studies.

Keywords: *Juglans regia*; anthracnose; *Colletotrichum*; phylogenomics; multilocus sequence typing; pathogenicity.

Introduction

Walnut (*Juglans regia* L.) is one of the most economically important nut crops cultivated in temperate regions worldwide and has gained increasing relevance in Europe following the expansion of intensive orchards and improved commercial cultivars [1]. In Italy, walnut production has increased considerably over the last decades, particularly in northern regions characterized by intensive commercial cultivation systems [2]. Along with this expansion, fungal diseases affecting fruit quality and orchard productivity have become increasingly important. Among these, anthracnose represents one of the major constraints to walnut production in several growing areas, where severe outbreaks can cause fruit rot, premature fruit drop, defoliation, and significant yield losses under favorable environmental conditions [3, 4]. Historically, walnut anthracnose has primarily been attributed to Ophiognomonia leptostyla, whereas bacterial blight symptoms are associated with Xanthomonas arboricola pv. *j*uglandis [5]. However, increasing evidence indicates that species of the genus Colletotrichum are among the major causal agents of anthracnose symptoms affecting walnut fruits, leaves, and reproductive tissues [6, 7]. Members of Colletotrichum represent one of the most important and taxonomically complex groups of plant pathogenic fungi worldwide, characterized by broad host ranges, variable pathogenic behavior, and extensive cryptic diversity [8, 9]. Advances in molecular systematics, together with the more recent application of phylogenomic approaches, have substantially improved species delimitation and taxonomic resolution within the genus, revealing that many morphologically similar isolates previously assigned to cosmopolitan taxa belong to distinct phylogenetic species complexes [10]. Species associated with walnut anthracnose belong mainly to the Acutatum and Gloeosporioides species complexes, although additional lineages

have occasionally been reported. In Europe, walnut infections have been associated predominantly with C. godetiae, C. fioriniae, and C. nymphaeae, whereas surveys conducted in Asia have revealed a broader diversity of pathogenic taxa, including C. fructicola, C. siamense, C. aenigma, C. sojae, and other closely related species [1, 3, 4]. In Italy, walnut anthracnose has so far been associated mainly with C. fioriniae and C. nymphaeae [6], while broader species diversity has been reported in France and Asia. Walnut anthracnose is increasingly recognized as a disease complex caused by multiple *Colletotrichum* species rather than by a single pathogen [11]. Defining the diversity of *Colletotrichum* species associated with walnut and all the other crops has therefore become a priority for improving disease diagnosis and management [12]. Continuous surveillance of commercial orchards is essential to detect newly emerging species and improve our knowledge of the diversity of pathogens associated with walnut [13]. Furthermore, because many *Colletotrichum* species are characterized by broad host ranges and have recently been reported on multiple fruit crops, understanding their occurrence in walnut orchards is important not only for walnut production but also for assessing the potential emergence and spread of pathogens across different agricultural systems [14]. Despite the increasing reports of walnut anthracnose caused by *Colletotrichum* spp. in Europe, comprehensive information on the diversity and distribution of *Colletotrichum* species associated with walnut remains limited. The occurrence of newly reported species and the taxonomic complexity of the genus highlight the need for accurate species identification, continuous monitoring, and assessment of their pathogenic potential [15]. These aspects are essential for improving disease diagnosis and for the early detection of pathogens that may threaten walnut production and other economically important fruit crops. Although multi-locus sequence typing (MLST) has substantially improved species delimitation within *Colletotrichum*, conventional barcoding loci may provide limited phylogenetic resolution when closely related taxa are compared [16]. Whole-genome sequencing and phylogenomic analyses provide a robust framework for validating species boundaries inferred from MLST and for establishing reliable genomic references for taxonomically complex genera such as *Colletotrichum* [17, 18]. While MLST remains an effective approach for routine species identification, genome-scale analyses offer increased phylogenetic resolution and generate genomic resources that will support

future comparative and population genomic investigations [19]. Differences in aggressiveness among *Colletotrichum* species may have important implications for disease management and risk assessment. However, comparative evaluations of the pathogenicity of walnut-associated *Colletotrichum* species are still limited, particularly in European production systems [1].

To address these knowledge gaps, a large-scale survey of walnut anthracnose was conducted between 2016 and 2024 in commercial orchards located in the Veneto region (Northern Italy), one of the main walnut-producing areas of the country. In this study, we investigated the diversity, phylogenetic relationships, and pathogenic variability of walnut-associated *Colletotrichum* species in Northern Italy through the integration of morphological characterization, multi-locus sequence typing, whole-genome sequencing, phylogenomic analyses, and pathogenicity assays. Specifically, our aims were to: (i) characterize the diversity of *Colletotrichum* species associated with walnut anthracnose in Northern Italy;(ii) confirm species identification using multilocus and phylogenomic approaches; (iii) evaluate the contribution of genome-scale phylogenomic analyses for validating species delimitation obtained through MLST; (iv) assess the pathogenicity and aggressiveness of representative species on walnut fruits.

Materials and Methods

Sampling and Isolation of Fungal Strains

From 2016 to August 2024, symptomatic samples were collected from commercial walnut orchards located in the eastern Po Valley (Veneto region, northern Italy), including the provinces of Padua, Rovigo, Treviso, and Venice. Sampling targeted fruits, buds, and stigmas of walnut trees showing typical symptoms of anthracnose. Plant tissues were plated onto acidified potato dextrose agar (PDA; Oxoid, Basingstoke, UK) amended with lactic acid (5%, v/v) to inhibit bacterial growth. Plates were incubated at 24 ± 2 °C for at least 6 days. Emerging fungal colonies were subcultured onto fresh PDA after 5–7 days. Isolates

125 preliminarily identified as belonging to the genus *Colletotrichum* based on colony
126 morphology were purified by single-spore isolation. Pure cultures were maintained on PDA
127 slants under mineral oil at 10 °C and in sterile distilled water at 4 °C in the fungal collections
128 of the Council for Agricultural Research and Economics – Plant Protection and Certification
129 (CREA-DC, Rome, Italy) and the University of Bologna (Italy). Detailed information on all
130 isolates included in this study is provided in Table 1.
131
132 Table 1. List of Colletotrichum sp. isolates analyzed in the present study, including host species and tissue
133 of isolation, together with their geographic origin in the Veneto region, Italy.

Isolate	**Host and Tissue**	**Geographic location**
CREADC-F2296	*Juglans regia* (nut)	Cittadella (PD) - Italy
CREADC-F2297	*Juglans regia* (nut)	Cittadella (PD) - Italy
CREADC-F2298	*Juglans regia* (nut)	San Donà di Piave (VE) - Italy
CREADC-F2303	*Juglans regia* (nut)	Cambio di Villadose (RO) - Italy
CREADC-F2372	*Juglans regia* (nut)	San Donà di Piave (VE) - Italy
CREADC-F2399	*Juglans regia* (nut)	Malspinoso (VI) - Italy
CREADC-F2421	*Juglans regia* (nut)	San Donà di Piave (VE) - Italy
CREADC-F2476	*Juglans regia* (bud)	San Donà di Piave (VE) - Italy
CREADC-F2478	*Juglans regia* (bud)	San Donà di Piave (VE) - Italy
CREADC-F2479	*Juglans regia* (bud)	Cittadella (PD) - Italy
CREADC-F2487	*Juglans regia* (stigma)	San Donà di Piave (VE) - Italy
CREADC-F2491	*Juglans regia* (stigma)	Cittadella (PD) - Italy
CREADC-F2270	*Juglans regia* (nut)	Castelguglielmo (RO) - Italy
CREADC-F2271	*Juglans regia* (nut)	Castelguglielmo (RO) - Italy
CREADC-F2259	*Juglans regia* (nut)	San Donà di Piave (VE) - Italy
CREADC-F2299	*Juglans regia* (nut)	Cambio di Villadose (RO - Italy
CREADC-F2307	*Juglans regia* (nut)	San Donà di Piave (VE) - Italy
CREADC-F2308	*Juglans regia* (nut)	San Donà di Piave (VE) - Italy
CREADC-F2317	*Juglans regia* (nut)	San Donà di Piave (VE) - Italy
CREADC-F2379	*Juglans regia* (nut)	San Donà di Piave (VE) - Italy
CREADC-F2385	*Juglans regia* (nut)	San Donà di Piave (VE) - Italy
CREADC-F2397	*Juglans regia* (nut)	San Donà di Piave (VE) - Italy
CREADC-F2452	*Juglans regia* (nut)	San Donà di Piave (VE) - Italy
CREADC-F2455	*Juglans regia* (nut)	Quarto d'Altino (VE) - Italy
CREADC-F2456	*Juglans regia* (nut)	Quarto d'Altino (VE) - Italy
CREADC-F2457	*Juglans regia* (nut)	Quarto d'Altino (VE) - Italy

CREADC-F2458	*Juglans regia* (nut)	Quarto d'Altino (VE) - Italy
CREADC-F2459	*Juglans regia* (nut)	Quarto d'Altino (VE) - Italy
CREADC-F2460	*Juglans regia* (nut)	Chiarano (TV) - Italy
CREADC-F2461	*Juglans regia* (nut)	Chiarano (TV) - Italy
CREADC-F2366	*Juglans regia* (nut)	San Donà di Piave (VE) - Italy
CREADC-F2471	*Juglans regia* (bud)	San Donà di Piave (VE) - Italy
CREADC-F2472	*Juglans regia* (bud)	Quarto d'Altino (VE) - Italy
CREADC-F2473	*Juglans regia* (bud)	Quarto d'Altino (VE) - Italy
CREADC-F2474	*Juglans regia* (bud)	Cittadella (PD) - Italy
CREADC-F2475	*Juglans regia* (bud)	San Donà di Piave (VE) - Italy
CREADC-F2488	*Juglans regia* (stigma)	San Donà di Piave (VE) - Italy
CREADC-F2490	*Juglans regia* (stigma)	Eraclea (VE) - Italy
CREADC-F2492	*Juglans regia* (stigma)	Quarto d'Altino (VE) - Italy
CREADC-F2493	*Juglans regia* (stigma)	Quarto d'Altino (VE) - Italy
CREADC-F2481	*Juglans regia* (bud)	Eraclea (VE) - Italy
CREADC-F2480	*Juglans regia* (bud)	Cittadella (PD) - Italy
C177	*Juglans regia* (nut)	Adria (RV) - Italy
C141	*Juglans regia* (leaf)	Adria (RV) - Italy

Morphological Characterization

Morphological and cultural characteristics of 44 *Colletotrichum* isolates were evaluated on PDA and synthetic nutrient-poor agar (SNA; Nirenberg, 1976). Cultures were incubated at 25 °C under a 12 h light/12 h dark photoperiod. After 7 days of incubation, colony morphology was assessed on PDA, including surface color, texture, zonation, margin characteristics, and reverse pigmentation. Observations were performed in triplicate, with two measurements per replicate. Microscopic observations were conducted using a Leica DM6 B light microscope (Leica Microsystems, USA). Conidial morphology was examined on SNA cultures. For each isolate, 30 randomly selected conidia were measured to determine length and width, and length/width ratios were calculated. Descriptive statistics, including mean, minimum, and maximum values, were recorded for each isolate, and the differences between the species were statistically evaluated using ANOVA analysis.

Genomic DNA extraction

Genomic DNA was extracted from fresh mycelium of 18 representative isolates selected for whole-genome sequencing (WGS) based on geographic origin, colony morphology, and

preliminary ITS-based identification, using a modified CTAB protocol [20]. Mycelium was scraped from culture plates using a sterile scalpel and transferred to sterile tubes containing beads (Zymo Research). A volume of 900 µL of 3% CTAB extraction buffer was added, and samples were homogenized using a Bioprep-24 homogenizer (AllSheng Instruments) at 4,500 rpm for 2 min. Samples were centrifuged at 12,000 rpm (13,225 × g) for 10 min at room temperature. The supernatant (700 µL) was transferred to a new 1.5 mL sterile tube, mixed with an equal volume of chloroform:isoamyl alcohol (24:1), and gently vortexed. Following centrifugation at 12,000 rpm for 10 min, 550 µL of the aqueous phase was transferred to a new tube, and DNA was precipitated by adding an equal volume of isopropanol. After centrifugation at 12,000 rpm for 10 min at 4 °C, the supernatant was discarded, and the DNA pellet was washed twice with 70% ethanol (5 min at 12,000 rpm, 4 °C). Pellets were air-dried under vacuum for 12 min and resuspended in 50 µL of 1× TE buffer. DNA samples were stored at −20 °C until further use.

For amplicon-based Sanger sequencing, genomic DNA was extracted from PDA-grown mycelium using the Wizard® Genomic DNA Purification Kit (Promega, Madison, WI, USA). Homogenization was performed using a TissueLyser II (Qiagen, Germany) at 30 Hz for two cycles of 30 s. DNA was eluted in 50 µL of rehydration buffer and stored at −20 °C. DNA concentration and purity were assessed using a NanoDrop ND-1000 spectrophotometer (Thermo Fisher Scientific, USA).

PCR amplification and Sanger sequencing

The internal transcribed spacer region of the nuclear ribosomal DNA (*ITS1–5.8S–ITS2*), a ~200 bp intron of the glyceraldehyde-3-phosphate dehydrogenase gene (*GAPDH*), and a partial fragment of the actin gene (*ACT*) were amplified using the primer pairs ITS1/ITS4 [21], GDF1/GDR1 [22], and ACT-512F/ACT-783R [23], respectively (Table 2).

PCR amplifications were performed using a GeneAmp® PCR System 9700 thermal cycler (Applied Biosystems, Foster City, CA, USA) in a total reaction volume of 12.5 µL. The PCR mixture contained 1 µL of 20× diluted genomic DNA, 0.2 µM of each primer, 1× PCR buffer (Bioline, Luckenwalde, Germany), 2 mM $MgCl_2$, 20 µM of each dNTP, 0.7 µL dimethyl sulfoxide (DMSO), and 0.25 U Taq DNA polymerase (Bioline).

Table 2. Primers and PCR cycles used in this study

Gene	Primers	Sequences (5'- 3')	Cycle
ITS	ITS1	TCCGTAGGTGAACCTGCGG	5′ at 95 °C, 30 x (1′ at 95 °C, 1′ at 55 °C, 1′ at 72 °C), 10′ at 72 °C
	ITS4	TCCTCCGCTTATTGATATGC	
GAPDH	GDF-F	GCCGTCAACGACCCCTTCATTGA	4′ at 95 °C, 30 x (30″ at 95 °C, 30″ at 57 °C, 45″ at 72 °C), 5′ at 72 °C
	GDR-R	GGGTGGAGTCGTACTTGAGCATGT	
ACT	ACT-512F	ATGTGCAAGGCCGGTTTCGC	4′ at 95 °C, 30 x (30″ at 95 °C, 30″ at 57 °C, 45″ at 72 °C), 5′ at 72 °C
	ACT-783R	TACGAGTCCTTCTGGCCCAT	

PCR products were separated by electrophoresis on 1% agarose gels in 0.5× Tris–borate–EDTA (TBE) buffer, stained with GelRed™ Nucleic Acid Gel Stain (Biotium, Hayward, CA, USA), and visualized under UV light. Gel images were acquired using a GelDoc 2000 system (Bio-Rad, Hercules, CA, USA). Prior to sequencing, PCR products were purified using the NucleoSpin® Extract II kit (Macherey-Nagel, Düren, Germany) according to the manufacturer's instructions. Purified amplicons were sequenced by Eurofins MWG (Ebersberg, Germany) using the same primers employed for PCR amplification.

Whole Genome Sequencing and Genome assembly

Genomic DNA was submitted to an external sequencing service for library preparation and Illumina sequencing of 18 representative isolates (Sequentia Biotech, Barcelona; Biomarker Technologies, Germany). Paired-end sequencing was performed on an Illumina NovaSeq 6000 platform using a 150 bp PE configuration. Raw read quality was assessed using FastQC v0.12.1 (Babraham Bioinformatics, Cambridge, UK). Adapter sequences and low-quality bases were trimmed using Trimmomatic v0.33 [24] when required. Filtered reads were assembled de novo using SPAdes v4.0.0 [25]. Genome assemblies were manually inspected and filtered using Geneious Prime v2024.0.2 (Biomatters Ltd., Auckland, New Zealand), and scaffolds shorter than 350 bp were discarded. Scaffolds showing very low read coverage were removed as potential contaminants. Scaffolds corresponding to mitochondrial DNA (mtDNA) and ribosomal DNA (rDNA) were identified by BLASTN v2.9.0 [26] searches using reference sequences from *Colletotrichum* spp. as queries. Assembly completeness was

evaluated using BUSCO v5.4.5 [27] with the sordariomycetes_odb10 dataset, and assembly statistics (Supplementary Table 1) were calculated using QUAST v5.2.0 [28].

Multi-Locus Sequence Typing analysis

For preliminary species complex assignment, *ITS* sequences obtained from both Sanger sequencing and genome assemblies were compared against the NCBI nucleotide database using the BLASTn algorithm (http://blast.ncbi.nlm.nih.gov). The closest matches retrieved from the database were used to infer species complex affiliation and guide locus selection for subsequent multilocus sequence typing (MLST) analyses. For isolates analyzed through Sanger sequencing, chromatograms were manually inspected and trimmed to remove low-quality regions prior to BLASTn comparison against the NCBI database. For whole-genome sequenced isolates, local BLAST databases were generated in Geneious Prime v2024.0.2 (Biomatters Ltd., Auckland, New Zealand) using the assembled genomes, and target loci were retrieved through local BLAST searches using representative reference sequences.

For isolates assigned to the Acutatum and Orchidearum species complexes, six loci (*ITS*, *GAPDH*, *TUB2*, *ACT*, *HIS-3*, and *CHS-1*) were analyzed, whereas isolates belonging to the Gloeosporioides species complex were characterized using six loci (*ITS, GAPDH, TUB2*, *CAL, GS*, and *ApMat*). Different outgroup taxa were selected according to the species complex under investigation. *C. magnum* CBS 519.97 was used as the outgroup for the Orchidearum species complex (COSC), *C. orchidophilum* CBS 632.80 for the Acutatum species complex (CASC), and *C. endophyticum* YN1A4 for the Gloeosporioides species complex (CGSC). Due to the large number of taxa included within the CGSC, phylogenetic reconstruction was performed using only closely related reference species rather than the entire complex, to improve tree resolution and interpretability.

For each gene, sequence alignments were performed using MAFFT v7.525 [29] and manually refined in Geneious Prime v2024.0.2 (Biomatters Ltd., Auckland, New Zealand) when necessary. The resulting multiple sequence alignments were exported to MEGA11 [30] to determine the optimal substitution model for each dataset and to calculate alignment statistics. Three concatenated alignments were subsequently generated in Geneious Prime v2024.0.2 (Biomatters Ltd., Auckland, New Zealand). Phylogenetic relationships were inferred using three complementary approaches: Approximate Maximum Likelihood (AML), Bayesian Inference (BI), and Randomized Axelerated Maximum Likelihood (RAxML). AML analyses were performed with FastTree v2.1.11 [31] using a Generalized Time-Reversible (GTR) model with 20 rate categories across sites. Bayesian analyses were conducted in

MrBayes v3.2.6 [32] with four Markov chain Monte Carlo (MCMC) chains run from random starting trees for 1,000,000 generations, sampling every 1,000 generations. The first 25% of sampled trees were discarded as burn-in, and posterior probabilities (PP) were calculated from the remaining trees. Maximum likelihood analyses were performed using RAxML v8.2.7 [33] under the GTR-CAT model with 1,000 bootstrap replicates.

Phylogenomic analysis

Forty available online genomes were selected based on the different species complexes (Supplementary Table X) and *Verticillium dahliae* was selected as outgroup. Analyses were performed following the pipeline described by [17] Menicucci et al. (2025), using Helixer [34] through the helixerlite GitHub repository (v25.5.27) (https://github.com/nextgenusfs/helixerlite) instead of AUGUSTUS. Predicted proteomes were clustered into orthologous groups using OrthoFinder v0.431 [35]. Single-copy orthogroups were identified, and protein sequences were aligned using MAFFT v7.525 [29], refined with Gblocks v0.91 [36], and concatenated using AMAS v0.98 [37]. Phylogenomic trees were reconstructed from the concatenated alignment using RAxML v8.2.11[33], FastTree v2.1.11 [31], and MrBayes v3.2.6 [32], with specific parameters as described by Menicucci et al. [17].

MLST characterization from whole-genome assemblies

To directly compare the phylogenomic and conventional MLST approaches, an additional multilocus phylogenetic analysis was performed using the same set of genomes included in the phylogenomic dataset. In addition to the isolates characterized in the present study, all reference genomes employed for the phylogenomic reconstruction were included in the MLST analysis. The loci commonly used for *Colletotrichum* species delimitation were manually extracted from each genome assembly and individually curated prior to alignment. Sequence alignments, concatenation, substitution model selection, and phylogenetic reconstructions were then carried out following the same procedures described above for the standard MLST analyses. This approach allowed a direct comparison between phylogenomic inference and MLST-based phylogenetic reconstruction using an identical taxon sampling. *Colletotrichum orbiculare* was used as the outgroup taxon.

Pathogenicity tests

Representative *Colletotrichum* isolates obtained in this study, including *C. fioriniae* (CREADC-F2317), *C. godetiae* (CREADC-F2271), *C. nymphaeae* (CREADC-F2372), *C. fructicola* (CREADC-F2480), *C. siamense* (CREADC-F2481), and *C. sojae* (C141), were selected for pathogenicity assays on artificially wounded walnut fruits. Fruits were surface sterilized in 1% (v/v) sodium hypochlorite for 1 min, rinsed with sterile distilled water, and air-dried on sterile paper towels. Each fruit was wounded on the pericarp using a sterile needle, and a 6-mm diameter agar plug taken from the margin of an actively growing colony was placed onto the wound, with the mycelium facing the fruit surface. Control fruits were wounded and inoculated with sterile PDA plugs without mycelium. Ten fruits were inoculated for each isolate, and the experiment was performed twice independently. Inoculated fruits were incubated in a moist chamber at 24 °C. Lesion development was monitored daily. Two perpendicular lesion diameters were measured 7 days after the first appearance of symptoms, corresponding 10 days after inoculation. Final lesion size data were subjected to analysis of variance (ANOVA), followed by Fisher's LSD post hoc test using Statgraphics Centurion (Statgraphics Technologies, USA). To fulfill Koch's postulates, fungi were re-isolated from symptomatic tissues onto PDA, and the resulting colonies were compared morphologically and molecularly with the original inoculated isolates.

Results

Sampling, Isolation, and Distribution of Fungal Isolates

In the present study, a total of 44 *Colletotrichum* isolates were collected from walnut fruits, buds, stigmas, and leaves. Most isolates originated from the Province of Venice (65.9%), followed by the Provinces of Padua and Rovigo, each accounting for 13.6% of the total isolates. Lower percentages were recorded for the Provinces of Treviso (4.5%) and Vicenza (2.3%). Regarding the tissue of origin, most isolates were obtained from nuts, representing 65.9% of the total, followed by buds (22.7%) and stigmas (9.1%), whereas only one isolate (2.3%) was recovered from leaves (Figure 1).



Fig. 1 Geographic distribution of *Colletotrichum* isolates collected from walnut anthracnose surveys in Northern Italy between 2016 and 2024. The map shows the proportion and number of isolates recovered from the main sampling provinces in the Veneto region, including Venice, Padua, Rovigo, Treviso, and Vicenza. Most isolates originated from the Province of Venice (65.9%, *n* = 29), followed by Padua and Rovigo (13.6%, *n* = 6 each), whereas lower frequencies were recorded in Treviso (4.5%, *n* = 2) and Vicenza (2.3%, *n* = 1). The inset bar chart summarizes the distribution of isolates according to the host tissue of origin, indicating that nuts represented the predominant source of isolation (65.9%), followed by buds (22.7%), stigmas (9.1%), and leaves (2.3%).

Multi-locus sequence typing analysis

Multi-locus sequence typing (MLST) analyses revealed a high degree of taxonomic diversity within the *Colletotrichum* population associated with walnut anthracnose in Northern Italy. Phylogenetic reconstruction based on concatenated loci assigned all isolates to three major *Colletotrichum* species complexes: C. Orchidearum (COSC), C. Gloeosporioides (CGSC), and C. Acutatum (CASC) species complexes (Figure 2, Figure 3, Figure 4).

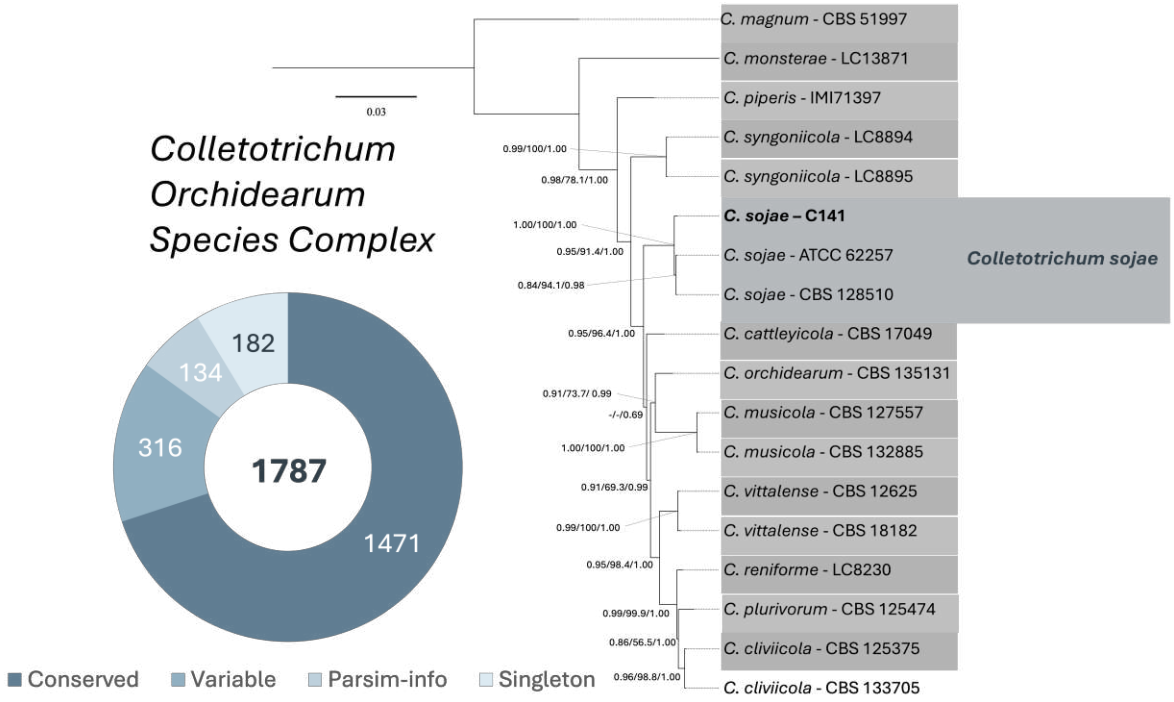

Fig. 2 Multi-locus sequence typing (MLST) phylogeny of the *Colletotrichum orchidearum* species complex and alignment statistics. The phylogenetic tree was reconstructed from concatenated loci using representative reference strains and the walnut isolate C141 obtained in this study. The isolate C141 clustered within the *C. sojae* clade together with ex-type and reference strains, confirming its taxonomic placement within the *C. orchidearum* species complex. The donut chart summarizes the characteristics of the concatenated alignment used for phylogenetic inference, showing the number of conserved, variable, parsimony-informative, and singleton sites. The analysis supports the identification of *C. sojae* as a member of the walnut-associated *Colletotrichum* population in Northern Italy.

Most isolates clustered within the CASC, which represented the dominant lineage recovered during the survey. Within this complex, 26 isolates were identified as *C. fioriniae*, 12 as *C. nymphaeae*, and 2 as *C. godetiae*. In addition, three isolates belonged to the CGSC, including two isolates identified as *C. fructicola* and one as *C. siamense.* Only one isolate belonged to the COSC and it was identified as *C. sojae*.

Phylogenetic analyses generated using Approximate Maximum Likelihood (AML), Bayesian Inference (BI), and RAxML approaches produced largely congruent topologies and supported the assignment of isolates to previously described species-level clades. Most taxa formed strongly supported monophyletic groups with corresponding reference strains retrieved from GenBank. However, the resolution obtained among closely related taxa varied across species complexes, with some internal branches showing limited statistical support, particularly within the CGSC.

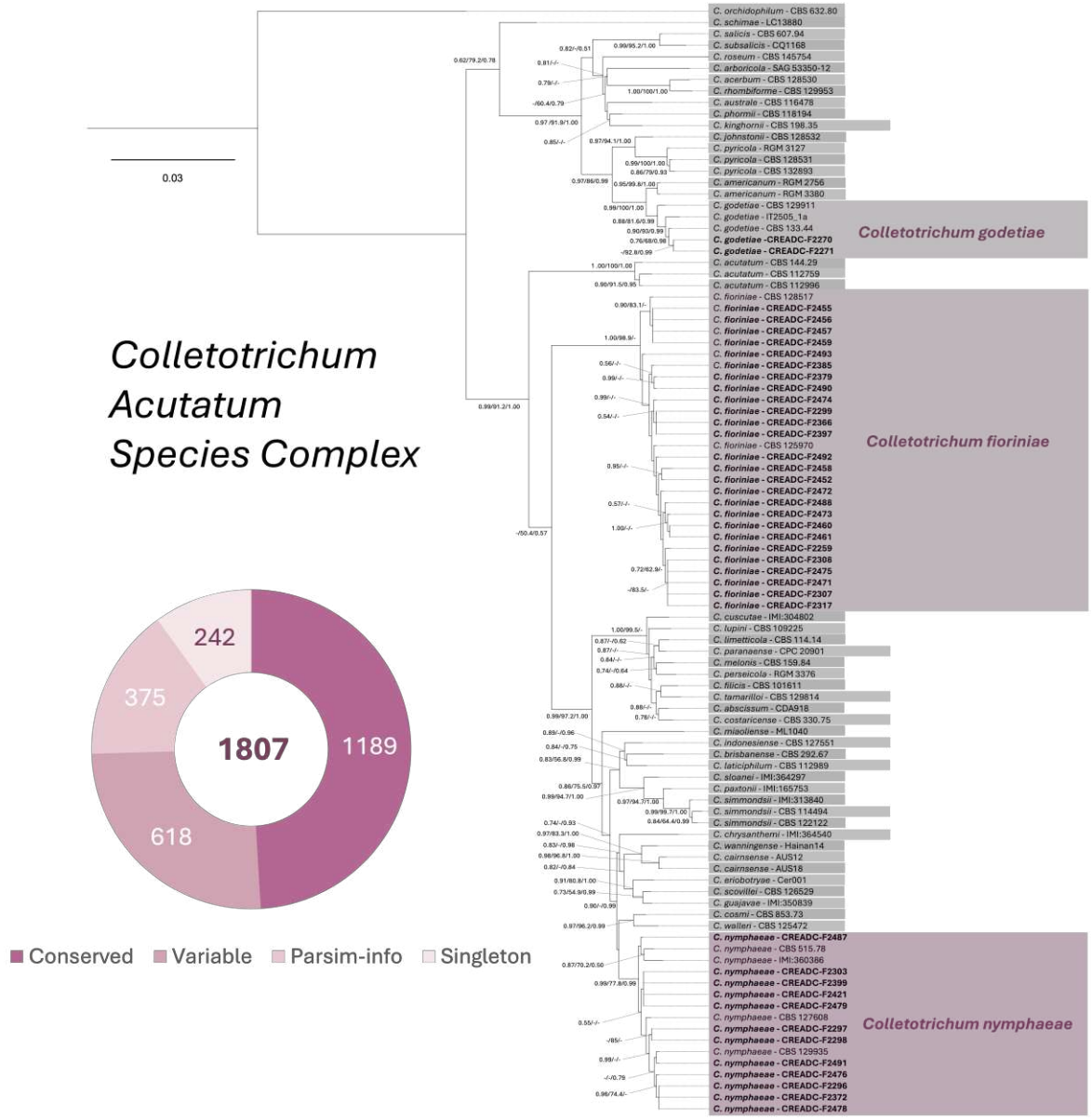

Fig. 3 Multi-locus sequence typing (MLST) phylogeny of the *Colletotrichum acutatum* species complex and alignment statistics. The phylogenetic tree was reconstructed from concatenated loci and includes reference strains together with walnut-associated isolates collected in Northern Italy. The analysis resolved three species within the *C. acutatum* species complex: *C. fioriniae*, *C. nymphaeae*, and *C. godetiae*. Most isolates clustered within the *C. fioriniae* clade, followed by *C. nymphaeae*, whereas only two isolates were assigned to *C. godetiae*. All identified taxa formed well-supported monophyletic groups with their corresponding reference strains, confirming species-level assignments. The donut chart summarizes the composition of the concatenated alignment, showing the number of conserved, variable, parsimony-informative, and singleton sites used for phylogenetic reconstruction. The results indicate that members of the *C. acutatum* species complex represent the predominant *Colletotrichum* lineage associated with walnut anthracnose in Northern Italy.

Overall, MLST analyses demonstrated that walnut anthracnose in Northern Italy is associated with a genetically heterogeneous assemblage of *Colletotrichum* taxa belonging to multiple phylogenetically distinct lineages rather than to a single dominant pathogen species.

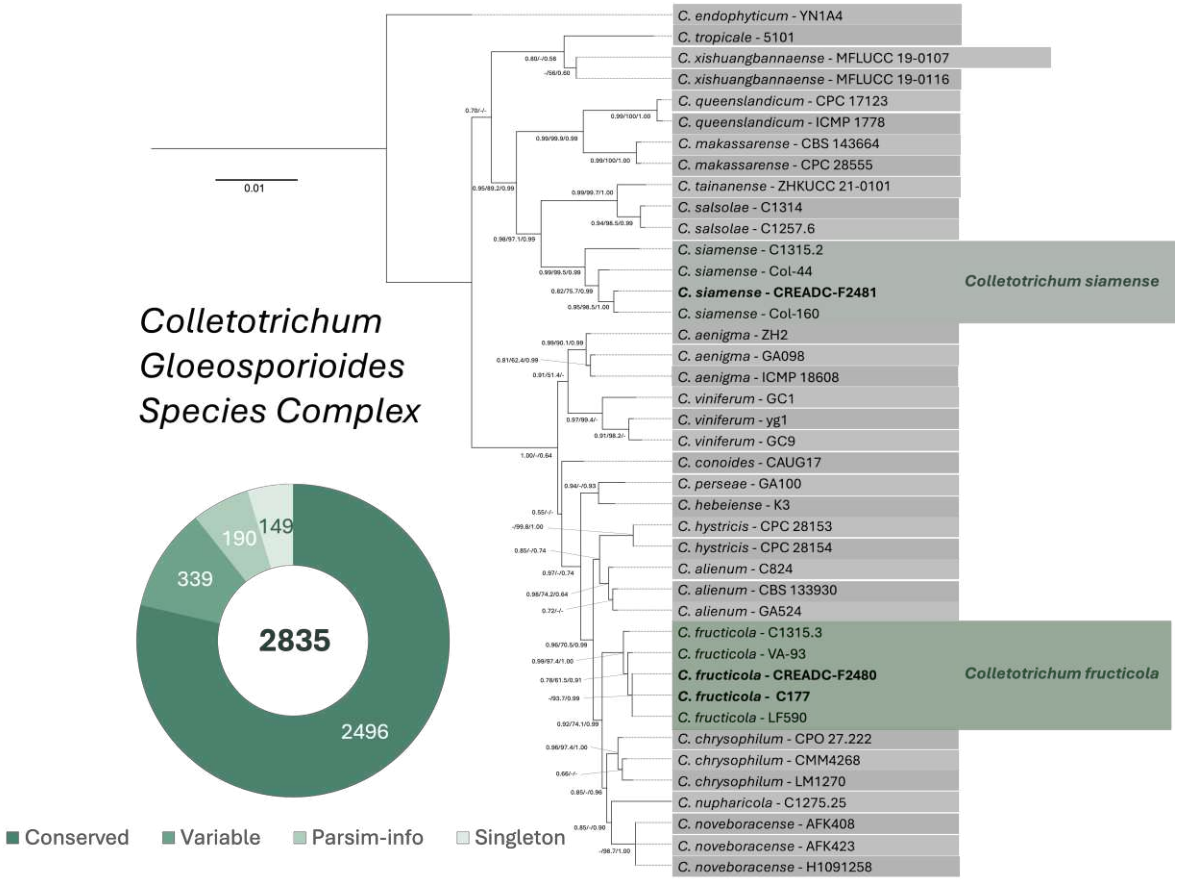

Fig. 4 Multi-locus sequence typing (MLST) phylogeny of the *Colletotrichum gloeosporioides* species complex and alignment statistics. The phylogenetic tree was reconstructed from concatenated loci and includes reference strains together with walnut-associated isolates collected in Northern Italy. The analysis identified two species belonging to the *C. gloeosporioides* species complex: *C. fructicola* and *C. siamense*. Two isolates (CREADC-F2480 and C177) clustered within the *C. fructicola* clade, whereas one isolate (CREADC-F2481) was assigned to *C. siamense*. All isolates grouped within well-supported monophyletic clades together with their corresponding reference strains, confirming their species-level identification. The donut chart summarizes the composition of the concatenated alignment used for phylogenetic reconstruction, showing the number of conserved, variable, parsimony-informative, and singleton sites. These results demonstrate the occurrence of members of the *C. gloeosporioides* species complex associated with walnut anthracnose in Northern Italy, including taxa that have only recently been reported on walnut in Europe.

Phylogenomic validation of MLST-based species delimitation

To achieve genome-scale validation of species identifications obtained through MLST, whole-genome sequencing was conducted on 18 representative *Colletotrichum* isolates associated with walnut. Phylogenomic analysis yielded a well-resolved tree in which all isolates clustered with their corresponding reference genomes, forming strongly supported monophyletic clades corresponding to *C. fioriniae*, *C. nymphaeae*, *C. godetiae*, *C. fructicola*, *C. siamense*, and *C. sojae* (Figure 5A). These results confirm the robustness of species assignments derived from multilocus sequence analyses and provide genome-scale support for the taxonomic placement of all representative isolates.

Phylogenomic Tree

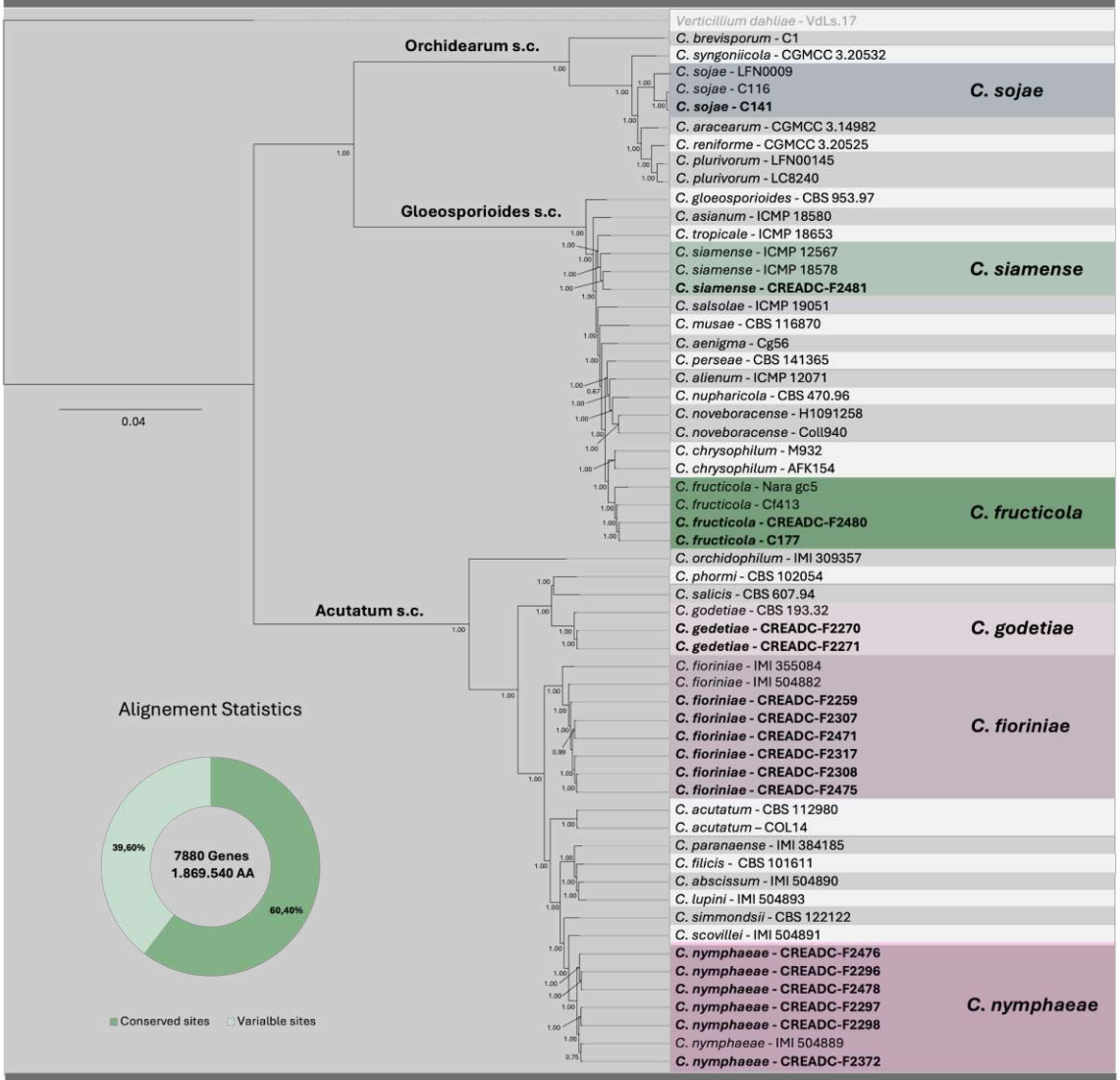

Tanglegram

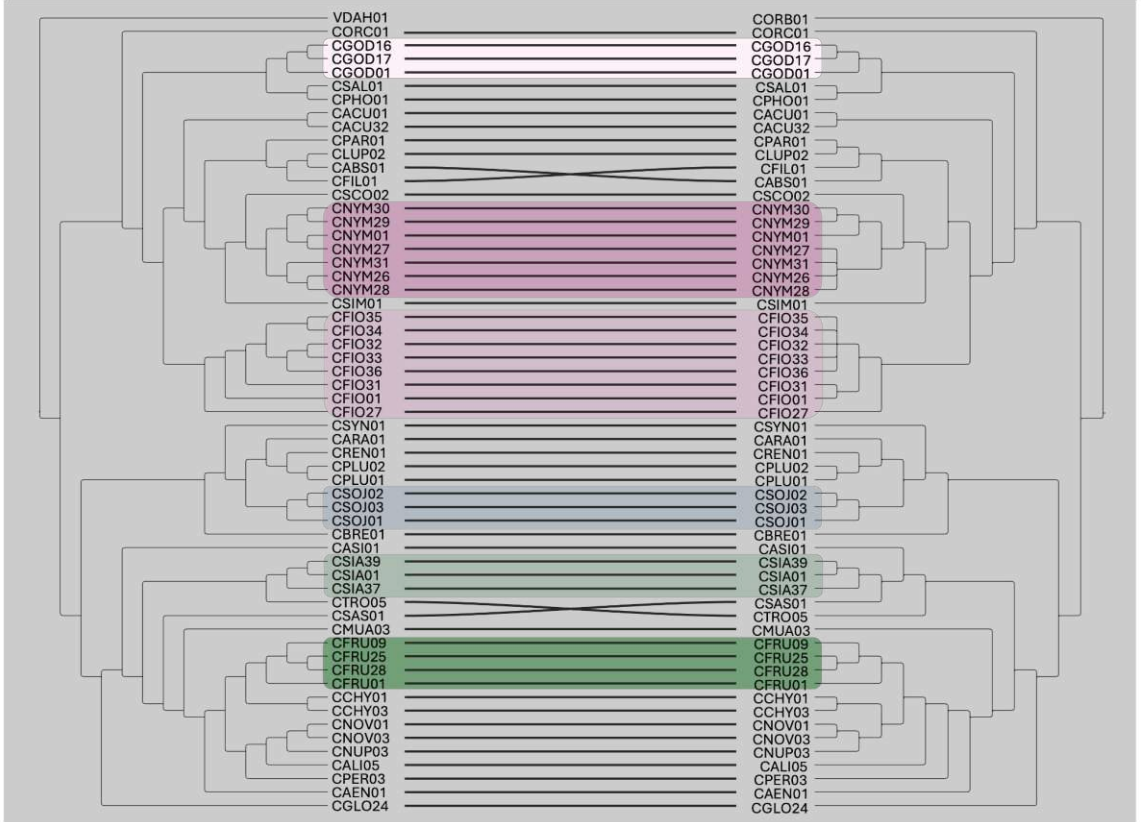

Fig. 5 Genome-scale phylogenomic validation of MLST-based species identification in walnut-associated *Colletotrichum*. **(A)** Phylogenomic tree reconstructed from genome-scale data, including representative isolates obtained in this study and reference genomes from different *Colletotrichum* species complexes. The analysis confirmed the species-level assignments inferred by MLST, with isolates identified as *C. fioriniae*, *C. nymphaeae*, *C. godetiae*, *C. fructicola*, *C. siamense*, and *C. sojae* clustering within well-supported monophyletic clades together with their corresponding reference genomes. **(B)** Tanglegram comparing the topology of the phylogenomic tree with that obtained from multilocus sequence typing (MLST) using the same taxon sampling. Connecting lines illustrate the correspondence between taxa in the two reconstructions and reveal a high degree of topological congruence. Only minor differences in the relative positions of a few closely related taxa were observed, highlighting the greater resolving power of genome-scale data while confirming the overall consistency of species delimitation obtained through MLST.

Comparison between phylogenomic reconstruction and the MLST-based phylogeny showed full agreement in species delimitation (Figure 5B). No differences in taxonomic assignment were observed between the two approaches, indicating that the multilocus markers employed in this study are sufficient for reliable species identification of walnut-associated *Colletotrichum*. However, the genome-scale dataset provided stronger phylogenetic support and enhanced resolution of relationships among closely related taxa, highlighting the value of phylogenomics as a robust framework for validating species boundaries and generating genomic resources for future comparative and population genomic studies.

Morphological characterization

Representative *Colletotrichum* isolates displayed colony morphologies consistent with their molecular identification. Differences in colony pigmentation, aerial mycelium development, and sporulation patterns were observed among species (Figure 6A), although these characteristics largely overlapped and were not sufficient for reliable species discrimination. Overall, morphological observations were consistent with the species assignments obtained through MLST and phylogenomic analyses. (Figure 6A).

Microscopic observations revealed moderate variation in conidial morphology among representative species (Figure 6B). Overall, isolates belonging to the *C. gloeosporioides* and *C. orchidearum* species complexes produced larger conidia than those of the *C. acutatum* species complex. Conidia were generally hyaline, smooth-walled, aseptate, and straight, although their size and shape differed among species. Detailed measurements are reported below in Table 3.

Table 3. Comparative morphological features of representative *Colletotrichum* species associated with walnut anthracnose.

Species	Colony appearance	Conidia	Mean conidial size (µm)
C. fioriniae	Salmon to pale vinaceous	Fusiform–cylindrical	11.2 × 3.4
C. godetiae	Grey, cottony	Cylindrical	13.5 × 3.9
C. nymphaeae	Grey with brighter reverse	Cylindrical–clavate	13.5 × 4.1
C. fructicola	Darkening with age	Cylindrical	13.2 × 4.2
C. siamense	Darkening with age	Cylindrical–oblong	12.8 × 4.0
C. sojae	Grey colonies	Slightly curved	14.1 × 4.3

409

410

411 **Pathogenic variability among walnut-associated *Colletotrichum* isolates**

412 Pathogenicity assays confirmed that all representative *Colletotrichum* species identified in
413 this study were able to infect walnut fruits and induce typical anthracnose symptoms under
414 controlled conditions. Necrotic lesions developed on all inoculated fruits within 10 days after
415 inoculation and progressively expanded throughout the incubation period, whereas no
416 symptoms were observed on the control fruits (Figure 6C).

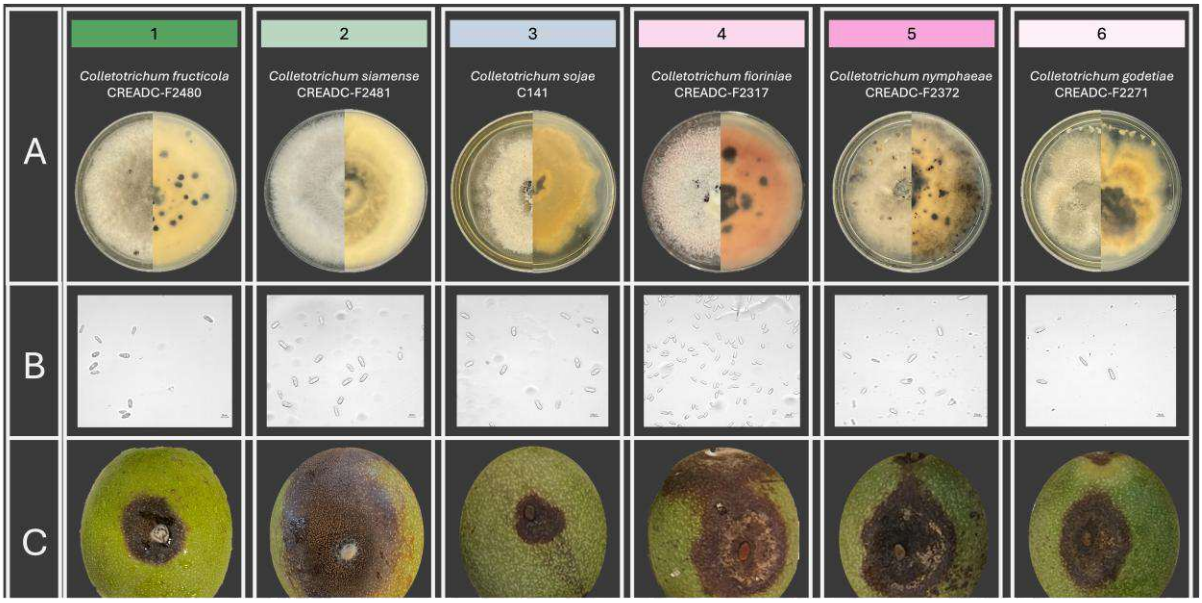

417

418 **Fig. 6 Morphological characteristics and pathogenicity of representative *Colletotrichum* species associated with**
419 **walnut anthracnose in Northern Italy. (A)** Colony morphology of representative isolates grown on potato dextrose agar

(PDA) after incubation under controlled conditions. For each isolate, both the upper (front) and lower (reverse) sides of the colony are shown, highlighting differences in colony texture, pigmentation, and sporulation patterns among species. **(B)** Microscopic observations of conidia produced by the corresponding isolates. Conidia were examined to assess morphological features, including size and shape, which varied among species but were generally hyaline, aseptate, and smooth-walled. **(C)** Representative symptoms produced in pathogenicity assays on artificially wounded walnut fruits ten days after inoculation. All tested isolates induced necrotic lesions of variable size and severity, confirming their pathogenicity on walnut. The figure includes representative isolates of *C. fructicola* (CREADC-F2480), *C. siamense* (CREADC-F2481), *C. sojae* (C141), *C. fioriniae* (CREADC-F2317), *C. nymphaeae* (CREADC-F2372), and *C. godetiae* (CREADC-F2271).

Analysis of lesion development revealed significant differences in lesion size among the tested isolates (ANOVA, $P < 0.05$) (Figure 7). Although all isolates were pathogenic, the extent of necrotic tissue varied among species. The tested *Colletotrichum nymphaeae isolate* produced the largest mean necrotic area under the experimental conditions. Intermediate lesion sizes were observed for *C. fructicola*, *C. fioriniae*, *C. godetiae*, *C. sojae*, and *C. siamense*, although lesion development differed among taxa. Overall, these results demonstrate that walnut anthracnose in northern Italy is associated with multiple pathogenic *Colletotrichum* species, with isolate-dependent differences in lesion development on wounded walnut fruits.

Fig. 7 Comparison of lesion development caused by representative walnut-associated *Colletotrichum* isolates. Bars represent the mean necrotic area (mm^2) measured on wounded walnut fruits 10 days after inoculation. Error bars indicate standard deviations. Different letters denote statistically significant differences according to Fisher's LSD test ($P < 0.05$). All tested isolates produced significantly larger lesions than the negative control, confirming their pathogenicity on walnut fruits.

Discussion

This study substantially advances the current knowledge of walnut-associated *Colletotrichum* in Europe by providing two major contributions. First, it considerably expands the currently known diversity of *Colletotrichum* associated with walnut in Europe through the identification of six pathogenic species, including *C. fructicola*, *C. siamense*, and *C. sojae*, which are reported here for the first time as causal agents of walnut anthracnose in Europe. Second, it provides robust genome-scale validation of species identification through whole-genome sequencing and phylogenomic analyses, generating a valuable genomic resource that will support future comparative and population genomic studies. Together, these findings reinforce the concept that walnut anthracnose is a complex disease caused by multiple

phylogenetically distinct *Colletotrichum* species rather than by a single dominant pathogen [1, 9].

The predominance of *C. fioriniae*, *C. nymphaeae*, and *C. godetiae* agrees with previous reports from Italy and other European countries [1, 6], confirming that these species remain the principal causal agents of walnut anthracnose in Europe. However, one of the major findings of this study is the identification of *C. fructicola*, *C. siamense*, and *C. sojae*, which substantially broadens the diversity of *Colletotrichum* currently known to be associated with walnut. Beyond representing the first European reports of these pathogens on walnut, these findings indicate that the composition of the walnut anthracnose pathosystem is more diverse than previously recognized and emphasize the importance of continuous surveillance programs aimed at detecting emerging pathogens. Interestingly, these same species have recently been reported on apple in the same geographical area [38]. Although the present study was not designed to investigate pathogen movement among hosts, their occurrence on different fruit crops suggests that walnut orchards should be considered within a broader agroecosystem context, where shared pathogen communities may contribute to future disease emergence.

An important outcome of this study is the generation of whole-genome sequences for 18 representative walnut-associated *Colletotrichum* isolates. Phylogenomic analyses consistently confirmed all species assignments previously obtained through MLST, providing robust genome-scale support for species delimitation across the principal *Colletotrichum* species complexes. This result demonstrates that the multilocus framework adopted in this study provides reliable species identification for walnut-associated *Colletotrichum*, while whole-genome sequencing offers a robust taxonomic framework for validating species boundaries, increasing confidence in the placement of closely related taxa, and generating valuable genomic resources [39, 17, 40]. As additional genome sequences from walnut-associated *Colletotrichum* isolates become available from different geographic regions, these data will facilitate comparative and population genomic studies aimed at reconstructing pathogen dispersal, host adaptation, and evolutionary history. Although these aspects were beyond the scope of the present study, the genomic resources generated here establish an important reference framework for future investigations.

Pathogenicity assays demonstrated that all representative *Colletotrichum* species identified in this study were pathogenic to walnut fruits under the experimental conditions adopted,

inducing typical anthracnose symptoms and fulfilling Koch's postulates. These findings support the pathogenic potential of the six species on wounded walnut fruits. Nevertheless, significant differences in lesion size were observed among the representative isolates. The tested *Colletotrichum nymphaeae isolate* produced the largest necrotic lesions under the conditions tested, whereas the remaining species induced intermediate or lower levels of disease severity. The tested *C. sojae* isolate induced lesions, but its aggressiveness relative to other isolates should not be generalized to the species lev*el*. These findings indicate pathogenic potential under experimental conditions, although the epidemiological roles of these taxa under natural orchard conditions remain to be established. Similar variability in pathogenicity among walnut-associated *Colletotrichum* species has also been reported in France [1], suggesting that disease severity may depend not only on species identity but also on differences in virulence among coexisting lineages. Understanding this variability will be important for improving disease risk assessment and developing effective management strategies.

Several limitations should be considered when interpreting these findings. The isolate collection was geographically uneven, with most isolates originating from the Province of Venice, and therefore may not fully represent *Colletotrichum* diversity across Northern Italy. Moreover, pathogenicity was assessed using one representative isolate per species on artificially wounded fruits. Consequently, the observed differences in lesion development cannot be generalized to species-level aggressiveness or natural infection conditions. Broader sampling, additional isolates per species, and assays on unwounded fruits and under field conditions will be needed to establish their epidemiological significance.

Overall, this study considerably extends the current knowledge of *Colletotrichum* diversity associated with walnut in Europe by combining extensive field surveys with integrative taxonomic and pathogenicity approaches. The integration of morphology, MLST, phylogenomics, and pathogenicity assays provides a robust framework for the identification and characterization of emerging *Colletotrichum* species associated with walnut. Furthermore, the discovery of newly reported pathogenic species together with the generation of genome-scale reference data establishes a valuable foundation for future surveillance programs and comparative and population genomic studies that will contribute to a deeper understanding of the evolution, dissemination, and epidemiology of walnut-associated *Colletotrichum* [9, 17].

References

1. Da Lio, D. et al. Combined metabarcoding and multi-locus approach for genetic characterization of *Colletotrichum* species associated with common walnut (*Juglans regia*) anthracnose in France. *Sci Rep*, **8**, 10765. https://doi.org/10.1038/s41598-018-29027-z (2018).

2. ISTAT-Italian National Institute of Statistics. Cultivations: Walnut http://dati.istat.it/Index.aspx?QueryId=33705. (2024).

3. Li, F. et al. Identification, pathogenicity, and sensitivity to fungicide of *Colletotrichum* species that causes walnut anthracnose in Beijing. *Agronomy*, **13**, 214 (2023).

4. Yu, X. et al. 4-Propylphenol Alters Membrane Integrity in Fungi Isolated from Walnut Anthracnose and Brown Spot. *J. of Fungi*, **11**, 610 (2025).

5. Giraud, M., & Verhaeghe, A. Fiche bio-agresseur: Anthracnose à *Colletotrichum* sp. en verger de noyers. *Arboric. Fruitière*, **2** (2015).

6. Luongo, L., Galli, M., Garaguso, I., Petrucci, M., & Vitale, S. First report of *Colletotrichum fioriniae* and *C. nymphaeae* as causal agents of anthracnose on walnut in Italy. *Plant Dis.*, **106**, https://doi.org/10.1094/PDIS-05-21-1062-PDN (2022).

7. Zhang, L., Zhao, L., Liang, C., Yu, L., & Zhang, Y. *Colletotrichum* species (Glomerellales, Glomerellaceae) causing walnut anthracnose in China. *MycoKeys*, **108**, 95 (2024).

8. Talhinhas, P., & Baroncelli, R. *Colletotrichum* species and complexes: geographic distribution, host range and conservation status. *Fungal Diversity*, **110**, 109-198 (2021).

9. Talhinhas, P., & Baroncelli, R. Hosts of *Colletotrichum*. *Mycosphere*, **14**, 158-261 (2023).

10. Cannon, P. F., Damm, U., Johnston, P. R., & Weir, B. S. *Colletotrichum*: current status and future directions. *Stud. Mycol*, **73**, 181-213 (2012).

11. Wang, Q. H. et al. Identification, virulence and fungicide sensitivity of *Colletotrichum gloeosporioides* s.s. responsible for walnut anthracnose disease in China. *Plant Dis.* **104**, 1358-1368 (2020).

12. Calì, M. et al. Emerging *Colletotrichum* Diseases on Apple in European Orchards: Challenges and Perspectives. *Plant Health Cases*, https://doi.org/10.1079/planthealthcases.2025.0018 (2025).

13. Piombo, E. et al. Metagenomics approaches the detection and surveillance of emerging and recurrent plant pathogens. *Microorganisms*, **9**, 188 (2021).

14. Baroncelli, R. et al. Gene family expansions and contractions are associated with host range in plant pathogens of the genus *Colletotrichum*. *BMC genomics*, **17**, 555 (2016).

15. McLaughlin, M. S., Abbasi, S., Abbasi, P. A., & Ali, S. Apple bitter rot and Glomerella leaf spot: A comprehensive review of causal species and their biology, fungicide sensitivities, and management strategies. *Plant Dis.* **108**, 3432-3445 (2024).

16. Jayawardena, R.S. et al. Notes on currently accepted species of *Colletotrichum*. *Mycosphere*, **7**, 1192–1260 (2016).

17. Menicucci, A. et al. Can whole genome sequencing resolve taxonomic ambiguities in fungi? The case study of *Colletotrichum* associated with ferns. *Front. Fungal Biol.* **6**, https://doi.org/10.3389/ffunb.2025.1540469 (2025).

18. Hyde, K. D. et al. The 2024 Outline of Fungi and fungus-like taxa. *Mycosphere*, **15**, 5146-6239 (2024).

19. Lücking, R. et al. Unambiguous identification of fungi: where do we stand and how accurate and precise is fungal DNA barcoding? *IMA fungus*, **11**, 14 https://doi.org/10.1186/s43008-020-00033-z (2020).

20. Prodi, A. et al. Difference in chemotype composition of *Fusarium graminearum* populations isolated from durum wheat in adjacent areas separated by the Apennines in Northern-Central Italy. *Plant Pathol. J.*, **27**, 354-359 (2011).

21. White, T. J., Bruns, T., Lee, S. J. W. T., & Taylor, J. Amplification and direct sequencing of fungal ribosomal RNA genes for phylogenetics. *PCR protocols: a guide to methods and applications*, **18**, 315-322 (1990).

22. Guerber, J. C., Liu, B., Correll, J. C., & Johnston, P. R. Characterization of diversity in *Colletotrichum acutatum* sensu lato by sequence analysis of two gene introns, mtDNA and intron RFLPs, and mating compatibility. *Mycologia*, **95**, 872-895 (2003).

575 23. Carbone, I., & Kohn, L. M. A method for designing primer sets for speciation studies
576 in filamentous ascomycetes. *Mycologia*, **91**, 553-556 (1999).

577 24. Bolger, A. M., Lohse, M., & Usadel, B. Trimmomatic: a flexible trimmer for Illumina
578 sequence data. *Bioinformatics*, **30**, 2114–2120 (2014).

579 25. Bankevich, A. et al. SPAdes: a new genome assembly algorithm and its applications
580 to single-cell sequencing. *J. Comput. Biol.*, **19**, 455-477 (2012).

581 26. Camacho, C. et al. BLAST+: architecture and applications. *BMC bioinformatics*, **10**,
582 421 (2009).

583 27. Simão, F. A., Waterhouse, R. M., Ioannidis, P., Kriventseva, E. V., & Zdobnov, E. M.
584 BUSCO: assessing genome assembly and annotation completeness with single-copy
585 orthologs. *Bioinformatics*, **31**, 3210-3212 (2015).

586 28. Gurevich, A., Saveliev, V., Vyahhi, N., & Tesler, G. QUAST: quality assessment tool
587 for genome assemblies. *Bioinformatics*, **29**, 1072-1075 (2013).

588 29. Katoh, K., & Standley, D. M. MAFFT multiple sequence alignment software version
589 7: improvements in performance and usability. *Mol. Biol. Evol.*, **30**, 772-780 (2013).

590 30. Tamura, K., Stecher, G., & Kumar, S. MEGA11: molecular evolutionary genetics
591 analysis version 11. *Mol. Biol. Evol.*, **38**, 3022-3027 (2021).

592 31. Price, M. N., Dehal, P. S., & Arkin, A. P. FastTree 2–approximately maximum-
593 likelihood trees for large alignments. *PloS one*, *5*(3), e9490 (2010).

594 32. Ronquist, F. et al. MrBayes 3.2: efficient Bayesian phylogenetic inference and model
595 choice across a large model space. *System. Biol.*, **61**, 539-542 (2012).

596 33. Stamatakis, A. RAxML version 8: a tool for phylogenetic analysis and post-analysis
597 of large phylogenies. *Bioinformatics*, **30**, 1312-1313 (2014).

598 34. Holst, F. et al. Helixer: ab initio prediction of primary eukaryotic gene models
599 combining deep learning and a hidden Markov model. *Nat. Methods* **23**, 732–739
600 https://doi.org/10.1038/s41592-025-02939-1 (2026).

601 35. Emms D. M.KellyS. OrthoFinder: phylogenetic orthology inference for comparative
602 genomics. *Genome Biol.*, **20**, 1–4 (2019).

36. Castresana J. Selection of conserved blocks from multiple alignments for their use in phylogenetic analysis. *Mol. Biol. Evol.*, **17**, 540–552 (2000).

37. Borowiec M. L. AMAS: a fast tool for alignment manipulation and computing of summary statistics. *PeerJ.*, **4**, e1660 (2016).

38. Calì, M. et al. Molecular and morphological insights into emerging *Colletotrichum* species causing apple bitter rot and Glomerella leaf spot in northern Italy. *Plant Dis.*, **109**, 2298-2308 (2025).

39. Kapli, P., Yang, Z., & Telford, M. J. Phylogenetic tree building in the genomic age. *Nat. Rev. Genet.*, **21**, 428–444 (2020).

40. Menicucci, A. et al. Adaptive genomic compartments shaped by giant mobile elements underpin the ancient emergence of fungal pathogenicity. *bioRxiv*, https://doi.org/10.64898/2026.05.11.723792 (2026).

Acknowledgments

The authors thank Mr. Antonio Fiorin (Noceto Soc. Coop.) and agronomist Alessio Signori for their technical support during field activities. The authors also thank Linda Bodavalli and Enrico Graffieti for laboratory assistance and Professor Antonio Prodi for technical and logistical support.

Author contributions

L. Luongo and S. Vitale conceived the study. S. Iacono, L. Luongo, I. Garaguso and I. Belleggia performed laboratory analyses. S. Iacono, I. Belleggia and A. Menicucci conducted phylogenomic analyses. S. Vitale and R. Bugiani coordinated field surveys and sampling activities. S. Iacono and L. Luongo wrote the first draft of the manuscript. R. Baroncelli and A. Menicucci, contributed to data interpretation and manuscript revision. All authors reviewed and approved the final version of the manuscript.

Data availability

The whole-genome assemblies generated in this study are available in the NCBI GenBank database under the accession numbers listed in Supplementary File 4. The sequences generated in this study are also available in the NCBI GenBank database, with the corresponding accession numbers listed in Supplementary File 3. The raw Illumina sequencing reads generated in this study are available in the NCBI Sequence Read Archive (SRA) under BioProject accession number PRJNA1458005 (https://www.ncbi.nlm.nih.gov/bioproject/PRJNA1458005), with the corresponding SRA accession numbers listed in Supplementary File 4.

Competing interests

The authors declare no competing interests.

Funding

This research received no external funding.

Ethics declarations

No human participants or animals were involved in this study.

Supplementary Files

This is a list of supplementary files associated with this preprint. Click to download.

- SupplementaryS1.xlsx
- SupplementaryS2.xlsx
- SupplementaryS3.xlsx